DOI: https://doi.org/10.24425/amm.2025.152508

Y.I. SUPRIYATNA[1,2**], W. ASTUTI[1], S. SUMARDI[1], A. PRASETYA[2,3], L.I. BR. GINTING[4], W. WAHAB[5], H.T.B. MURTI PETRUS[2,3*]

TITANIUM DIOXIDE PRODUCTION FROM LOW-GRADE ILMENITE ORE: MINERAL CHARACTERIZATION AND OPTIMIZATION

The characterization of low-grade ilmenite ore from Banten (Indonesia) is investigated, as well as the effects of particle size, NaOH:Ti ratio, and fusion time on Ti and Fe content in TiO_2 products. Mineral separation of low-grade ilmenite ore was performed using wet gravity, followed by sieving. Each sample size's magnetization (using 10,000 Gauss magnets) is followed by weighing the magnetization results. The sifted and magnetized samples were then analyzed with XRF for composition analysis and XRD for compound determination. FE-SEM was applied to analyze morphology. A microscope was used for metalografi analysis. The fusion temperature of the optimization process was determined using STA. Fusion times were 10, 30, 60, 90, and 150 minutes at 850°C, with a NaOH:Ti ratio (w/w) of 1:2, 2:1, and 4:1, and particle sizes of 0.177-0.149 mm, 0.149-0.105 mm, and 0.105-0.074 mm. The minerals ilmenite ($FeTiO_3$), magnetite (Fe_3O_4), and coesite (SiO_2) dominate the characterization of Banten low-grade ilmenite ore. Sixty minutes of fusion at 850°C with a 2:1 NaOH:Ti ratio (w/w) and 0.177-0.149 mm with 94.44% TiO_2 in a product was optimal.

Keywords: Caustic fusion; low-grade ilmenite; mineral characterization; optimization; annova; titanium dioxide

1. Introduction

Mineral resources of ilmenite ($FeTiO_3$) were discovered in Indonesia as a type of cassiterite-associated minerals at the Bangka Belitung Islands, as well as along the southern coast of Java island in the form of iron sands and groups of zircon sand mineral ($ZrSiO_4$) at Central Kalimantan [1-4]. Bangka ilmenite is a high-grade ilmenite ore. Low-grade ilmenite ore is Java island ilmenite (iron sand) and zircon sand mineral. Ilmenite is a raw material that can be used to make titanium metal, iron metal, and titanium dioxide (TiO_2) [5-8].

The chloride and sulfate processes are the two commercial methods for producing TiO_2 [6,9]. The sulfate process can use low-grade raw materials, but the product quality is inferior, and a significant quantity of iron sulfate waste is generated [10]. The chloride process can produce high-quality TiO_2 products, but it requires rare and expensive raw materials (natural rutile, leucoxene, and titania slag) [10,11]. Because natural rutile reserves are only 1-10% of ilmenite reserves, alternative processes for producing high-quality TiO_2 from low-grade ores are required [12,13].

Low-grade ores are typically processed into slag and sulfate [10,14,15]. Nonetheless, these processes are harmful to the environment, expensive, and generate a lot of waste or recycling. Furthermore, the slagging process consumes more energy, emits more greenhouse gases, and cannot treat radioactive ores [16-20]. Low-grade ilmenite ores have not been investigated for processing into TiO_2 in Indonesia. Impurities in low-grade ilmenite ore include Al_2O_3, CaO, MgO, MnO, V_2O_5, and SiO_2. As a result, it is essential to create an appropriate and environmentally friendly process for producing high-purity TiO_2.

Titanomagnetite is a low-grade ilmenite ore. Titanomagnetites can be found in a variety of titaniferous reserves, such as placer iron ore reserves all around the world. They are found primarily in ores as iron oxide minerals alongside magnetite, and they frequently join igneous intrusions of bare rocks, primarily

[1] RESEARCH CENTER OF MINING TECHNOLOGY, NATIONAL RESEARCH AND INOVATION AGENCY (PRTPB-BRIN), JL IR SUTAMI KM 15 TANJUNG BINTANG, SOUTH LAMPUNG 35361, INDONESIA
[2] GADJAH MADA UNIVERSITY, DEPARTMENT OF CHEMICAL ENGINEERING (SUSTAINABLE MINERAL PROCESSING RESEARCH GROUP), FACULTY OF ENGINEERING, JALAN GRAFIKA NO. 2 KAMPUS UGM BULAKSUMUR, D. I. YOGYAKARTA 55281, INDONESIA
[3] UNCONVENTIONAL GEO-RESOURCES RESEARCH CENTER, FACULTY OF ENGINEERING, UGM, JL. GRAFIKA NO. 2, KAMPUS UGM, YOGYAKARTA, 55281 INDONESIA
[4] DEPARTMENT OF MATERIAL AND METALLURGICAL ENGINEERING, KALIMANTAN INSTITUTE OF TECHNOLOGY, JL. SOEKARNO-HATTA KM. 15, KARANG JOANG, BALIKPAPAN, EAST KALIMANTAN, 76127, INDONESIA
[5] DEPARTMENT OF MINING ENGINEERING, FACULTY OF EARTH SCIENCE AND TECHNOLOGY, HALU OLEO UNIVERSITY, KAMPUS HIJAU BUMI TRIDHARMA, ANDUONOHU, KENDARI, SOUTHEAST SULAWESI, 93232, INDONESIA

Corresponding authors: * – bayupetrus@ugm.ac.id; ** – yayat_iman@yahoo.com

anorthosites. A few titaniferous ores contain sufficient iron to enable for next handling immediately after milling [21,22]. However, most ores must be upgraded, mainly if they posses ilmenite, vanadium, or other valuable components. The vanadium content of the magnetite and titanomagnetite concentrates obtained is high. Ilmenite and pyrite are differentiated from the non-magnetic fraction and regained through selective flotation into a variety of valuable products [23]. Several studies have used gravitational, magnetic, and electrostatic separation to process low-grade titanium ores. Synthetic rutile is produced using solid reduction processes such as the Becher, Benelite, Murso, Dunn, Kataoka, and Austpac processes, which convert iron into dissolved iron or its elemental form through high-temperature reduction followed by acid leaching to produce synthetic rutile [24-27]. This upgraded and produced TiO_2 process, on the other hand, requires five stages: beneficiation (wet/dry gravity and magnetization), high-temperature oxidation, reduction (which requires the use of a reductant (coal or coke), aeration, and acid leaching [28-32]. These processes, apart from requiring high temperatures, also require reducing agents, which are not environmentally friendly because they produce air pollution. Therefore, it requires the conversion of existing methods to be more environmentally friendly and cost-effective.

This research presents a novel method for producing titanium dioxide from low-grade ilmenite ores. Wet gravity and magnetic separation are the initial preparations. Furthermore, the process of fusion of ilmenite ore with solid sodium hydroxide at a temperature below 900°C. The fusion product is water-leached, hydrolyzed with water, and acid-leached with hydrochloric acid. The aim is to establish and optimize an alternative route to the traditional chloride route.

2. Experimental

2.1. Materials

Rancecet, Banten, Indonesia, supplied the ilmenite sample. NaOH P.A. (99%, Merck, Darmstadt, Germany) was used as the chemical.

2.2. Methods

Two kilograms of Ilmenite Banten were separated using wet gravity, followed by sying with fractions of >0.177 mm, 0.177-0.149 mm, 0.105-0.074 mm, 0.074-0.044 mm, and 0.044 mm. Ten thousand gauss magnets were used for magnetization. The magnetization results for each sample size are then weighed. Sifted and magnetized samples were therefore analyzed using XRF (PANalytical Epsilon^{3}XLE) with total time of 20 min and XRD (PANalytical X'Pert^3 Powder) with a total scan time of 6 min for Cu radiation over a 2θ range of 10-80° to identify the compounds. FE-SEM (Thermo scientific Quatro S) was applied to analyze morphology. A Nikon ECLIPSE 50i POL microscope was used for metalografi analysis. Simultaneous Thermal Analysis (STA) 449 F3 Jupiter was used in conjunction with NETZSCH QMS 403 Aeolos. The ANOVA method is used to determine which variables significantly influence the quality of TiO_2 products.

2.3. Experimental procedure

2.3.1. Decomposition

Each fusion experiment used approximately 50 g of ilmenite. The particle size effect was tested using three particle sizes (0.177-0.149 mm, 0.149-0.105 mm, and 0.105-0.074 mm). The weight ratio of NaOH to Ti varied between 0.5, 2, and 4. Fusion times were set at 10, 30, 60, 90, and 150 minutes. Fusion was conducted at 850°C with and without caustic soda. The homogeneous fusion mixture is transferred to an S.S. container and placed in a muffle furnace preheated to a predetermined temperature. The crucible was removed after the required fusion time and allowed to cool to room temperature before being weighed.

2.3.2. Fusion Product

Water was used to leach the fusion products to release any residual NaOH and hydrolyze the products, enabling the NaOH reactant to be recovered. Water was used to wash the hydrolyzed solids. During the process, some impurities were also removed.

2.3.3. Leaching

The leaching reagent was 20% hydrochloric acid with a 4-hour leaching time. The solution was tested for titanium and iron using ICP-OES. The solid product was dried and calcined. Following that, XRF was employed to identify the chemical elements contained in TiO_2 and XRD to investigate the TiO_2 compound. A Thermo Scientific Quatro S was utilized to examine the morphology.

3. Results and discussion

3.1. Ilmenite sample characterization

The weight distribution results according to the particle size and magnetization steps are shown in TABLE 1. This study's magnetization distribution of the Banten ilmenite samples was 85% magnetic.

Referring to TABLE 2, the Ti and Fe contents of Banten ilmenite samples tend to decrease as particle size decreases. Besides the Fe, Al, and Si content, which is more than 1%, other impurities are Mg, Mn, P, Ca, V, and Cr, which are less than 1%. TABLE 2 shows that wet gravity, sieving, and magnetic separa-

TABLE 1

The weight distribution due to particle size and magnetization

Particle size (mm)	Mass (% wt)	Magnetic (% wt)	Non-Magnetic (% wt)
>0.177	46.71	85.69	14.31
0.177-0.149	5.65	89.42	10.58
0.149-0.105	33.32	96.94	3.06
0.105-0.074	8.44	96.53	3.47
0.074-0.044	1.53	96.03	3.97
<0.044	4.35	100.00	0.00

tion processes can increase the Ti content while significantly reducing the Al, Si, and Ca contents of ilmenite concentrate (for particle sizes >0.177 mm to 0.105-0.074 mm). In contrast, the results for particle sizes 0.074-0.044 mm and <0.044 mm are inversely proportional.

The standard method involves slashing magnetic and non-magnetic samples and attaching them to a glass medium. Lighting from below is used for microscopic observations. Non-metallic minerals are more pronounced and lighter in color than metal minerals (Fig. 1). The metallographic analysis revealed that magnetic samples contained many metals (Fig. 1a), whereas non-magnetic samples contained many non-metallic elements (Fig. 1b).

The overlay SEM+EDS results in Fig. 2(a-f) confirmed that Ti and Fe were all coupled. Content of Ti and Fe share a similar propensity and distribution. According to EDS, the dominant elements at each particle size are Fe and Ti. Figs. 2a to 2f show that the particle size is getting smaller according to the sieving results.

The XRD pattern (Fig. 3) revealed two distinct pattern groups. The first group produced similar reports for particle sizes >0.177, 0.177-0.0149 mm, 0.177-0.0149 mm, and 0.105-0.074 mm. The particle sizes in the second pattern group were 0.074-0.044 mm and <0.044 mm, respectively. HighScore Plus (HSP) application evaluation for the initial group in Fig. 3 reveals that the prominent compounds found in Banten ilmenite are ilmenite ($FeTiO_3$) and magnetite (Fe_3O_4). The dominant compounds in the second group are ilmenite ($FeTiO_3$), magnetite (Fe_3O_4), and coesite (SiO_2).

TABLE 2

XRF analyses of raw materials and magnetic ilmenite concentrates for each particle size concentrate

Element	Content (% wt)						
	Raw	>0.177 mm	0.177-0.149 mm	0.149-0.105 mm	0.105-0.074 mm	0.074-0.044 mm	<0.044 mm
MgO	0.801	0.801	0.777	0.747	0.762	0.877	0.881
Al_2O_3	2.603	1.174	1.064	1.065	1.058	1.781	1.810
SiO_2	15.854	2.859	2.464	2.245	2.305	5.725	10.079
P_2O_5	0.289	0.512	0.498	0.492	0.469	0.497	0.532
CaO	18.846	0.939	0.813	0.754	0.725	2.580	3.239
TiO_2	22.067	35.926	36.605	36.734	36.632	31.643	30.188
V_2O_5	0.257	0.421	0.426	0.423	0.429	0.427	0.386
Cr_2O_3	0.033	0.033	0.031	0.028	0.028	0.042	0.050
MnO	0.855	0.845	0.853	0.859	0.868	0.826	0.780
Fe_2O_3	38.346	55.919	55.943	56.069	56.008	54.735	51.138

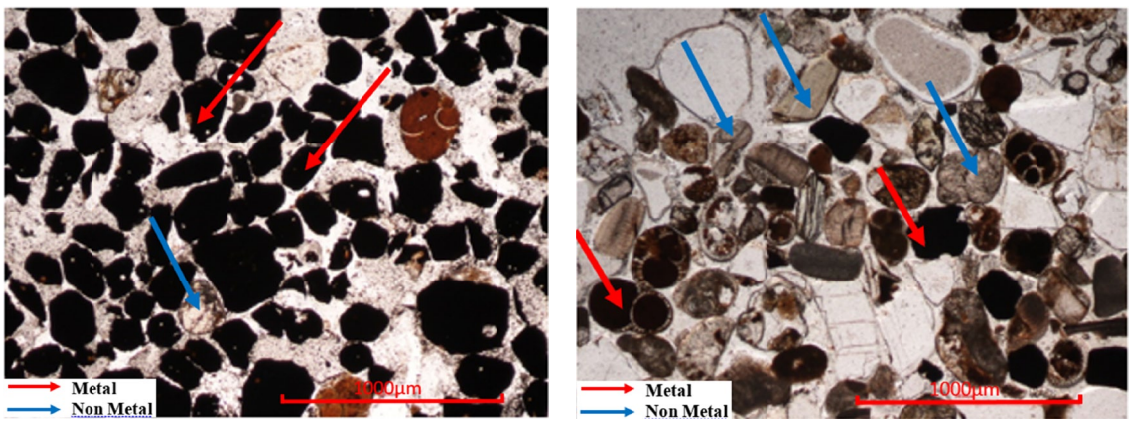

(a) magnetic (b) non-magnetic

Fig. 1. Metallographic analysis of magnetic and non-magnetic sample

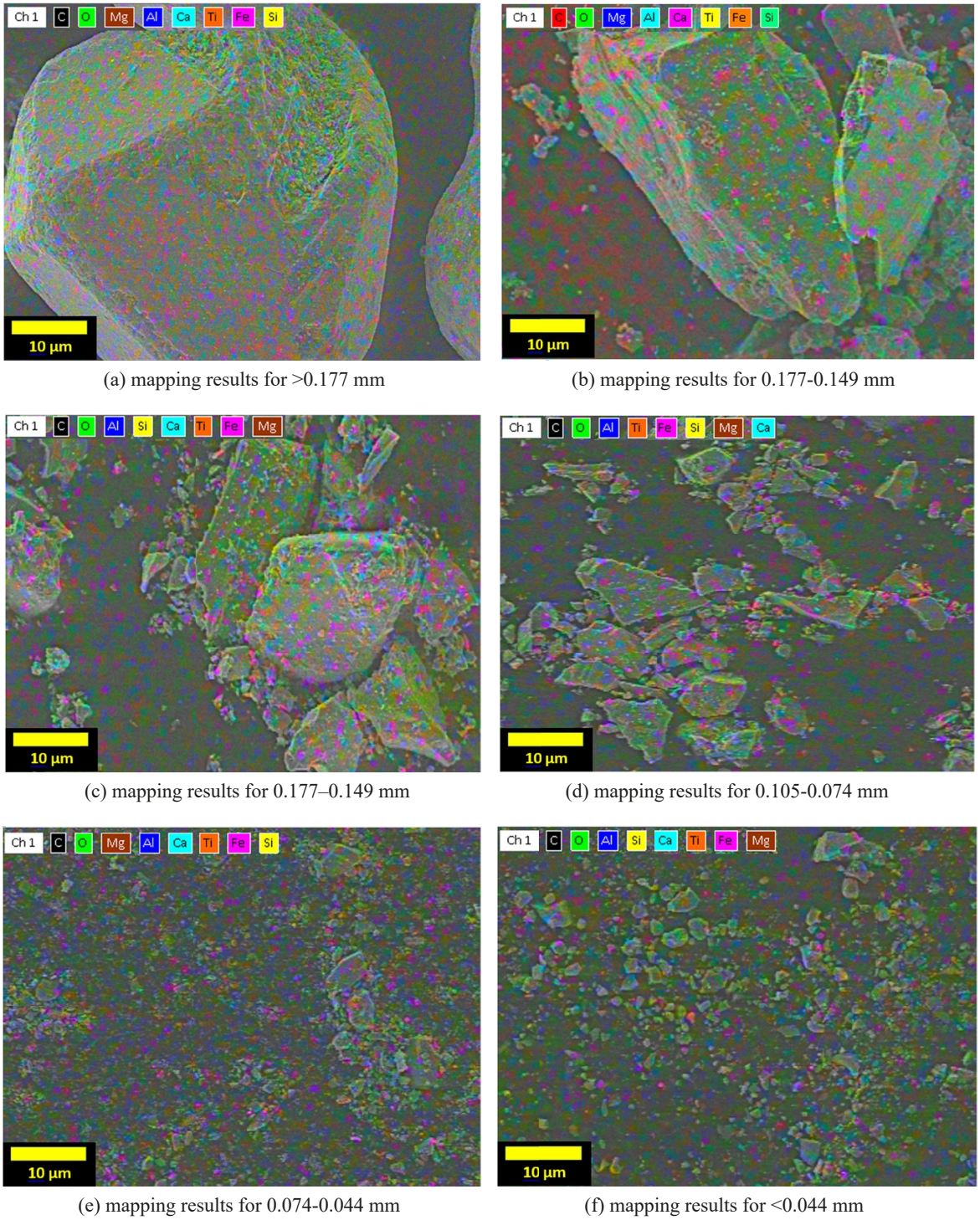

(a) mapping results for >0.177 mm

(b) mapping results for 0.177-0.149 mm

(c) mapping results for 0.177–0.149 mm

(d) mapping results for 0.105-0.074 mm

(e) mapping results for 0.074-0.044 mm

(f) mapping results for <0.044 mm

Fig. 2. Overlay SEM and EDS analysis for each particle size of the Banten ilmenite sample

3.2. TGA/DTA-DSC for the fusion process

The TG and DSC analysis results for the three particle sizes are nearly identical (Fig. 4). Based on the TG results, three intervals of change in sample weight occur. The first interval occurs at temperatures ranging from 25 to 700°C, with weight reductions of 4.13484% (0.177-0.149 mm), 4.32418% (0.149-0.105 mm), and 4.40034% (0.105-0.074 mm). Second interval at 700-1000°C with weight gains of 0.149482% (0.177-0.149 mm), 0.051694% (0.149-0.105 mm), and 0.110696% (0.105-0.074 mm). The third interval was between 1000 and 1200°C, with weight changes of 0.197392% (0.177-0.149 mm), 0.213688% (0.177-0.149 mm), and 0.175334% (0.105-0.074 mm). The DSC results revealed that the highest enthalpy data were found in the second interval, with values of 493.08 J/g (0.177-0.149 mm), 947.94 J/g (0.177-0.149 mm), and 946.87 J/g (0.105-0.074 mm).

Fig. 5(a) depicts the TG-MS measurement of sample 2B (ilmenite ore 0.177-0.149 mm reaction with NaOH) after heating to 1000°C in an inert atmosphere. The sample showed three mass loss steps of 16.9%, 4.8%, and 0.3%, with DTG signal peaks

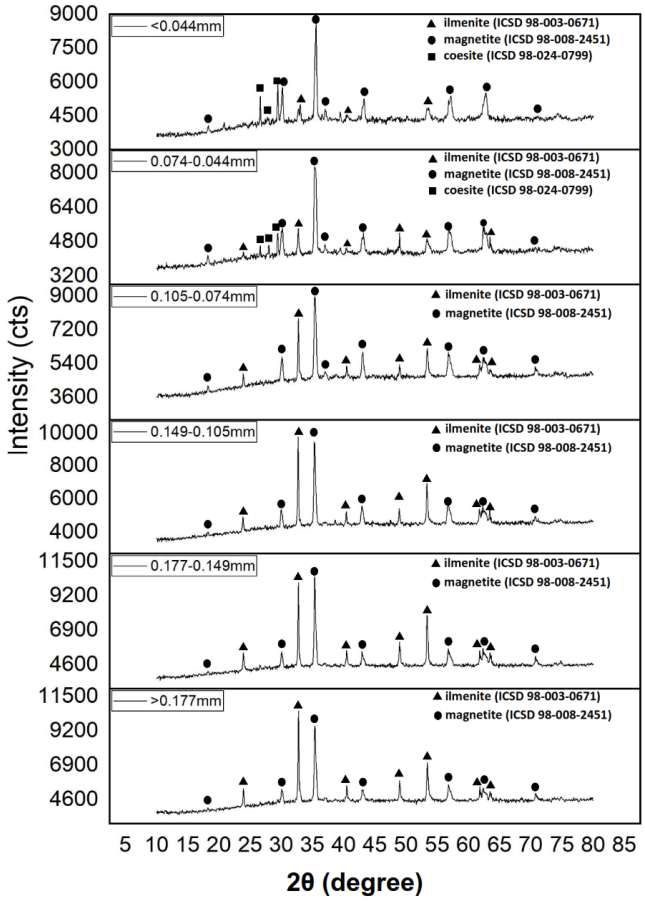

Fig. 3. The XRD pattern at different sizes of particles

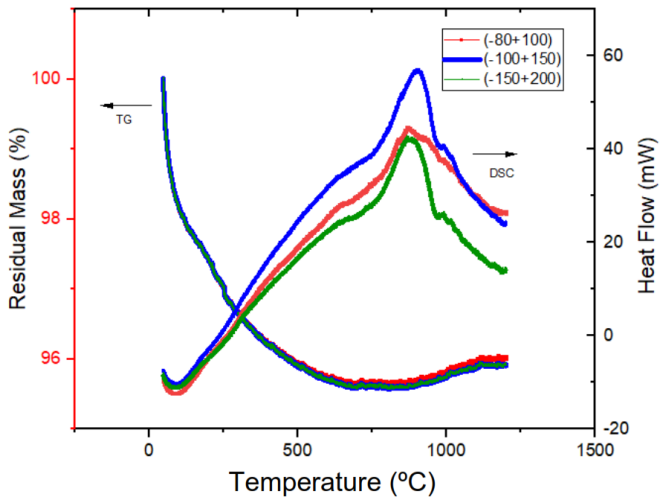

Fig. 4. TG and DSC curves of ilmenite ore in different particle size

at 163°C, 258°C, 631°C, and 857°C. The mass spectrometer detected an increase in mass numbers 18 (probably water), 44 (CO_2), 28, and 32 (fragments of water and CO_2). The release of water caused the first two steps in the mass loss. The release of CO_2 caused the third step. Fig. 5(b) shows similar results for samples sample 3B (ilmenite ore 0.105-0.074 mm reaction with NaOH). There were also three mass loss steps discovered, as well as the release of water and CO_2. The optimization process is carried out at 850°C based on the results of TG and DSC.

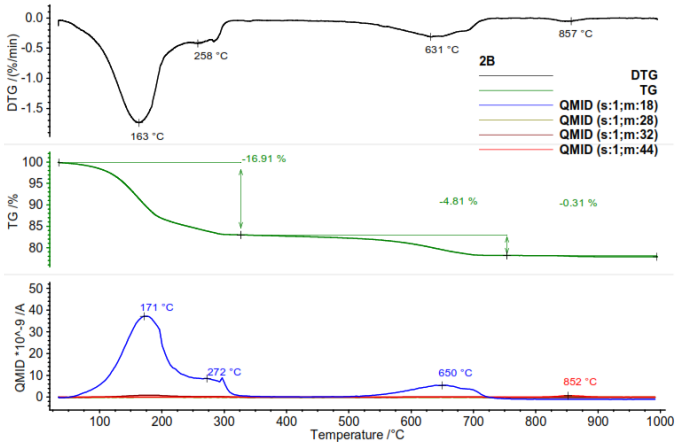

(a)

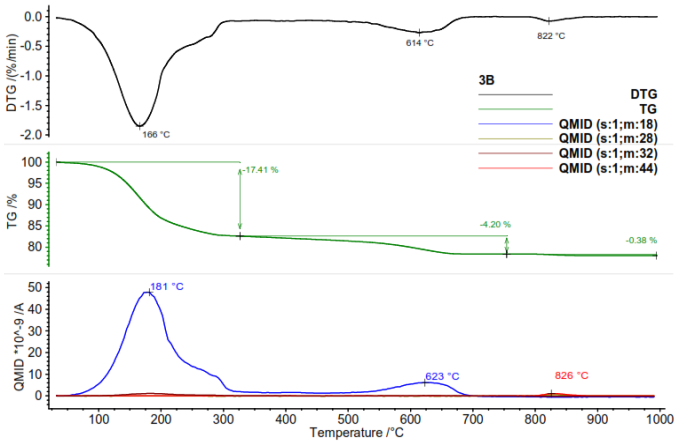

(b)

Fig. 5. TG, DTG, and mass number curve (a) ilmenite ore (0.177-0.149 mm), (b) ilmenite ore (0.105-0.074 mm) reaction with NaOH (10°C/minutes in oxygen)

3.3. Optimization of the fusion process

3.3.1. Effect of particle size, NaOH: Ti ratio, and fusion time

The effect of particle size on Ti content in TiO_2 products is shown in Fig. 6(a and c). At a fixed NaOH:Ti (w/w) ratio (2:1) and several fusion times shown in Fig. 6(a), it shows that the Ti contents are almost the same for the three particle sizes at the same fusion time. The effect of particle size for several NaOH:Ti ratios (w/w) in Fig. 6(c) shows the same thing: at the same ratio, the particle size does not significantly affect the Ti content in the TiO_2 product. The effect of the NaOH:Ti ratio (w/w) on the Ti content in the TiO_2 product is shown in Fig. 6(b and c). In Fig. 6(b), it can be seen that as the ratio of NaOH:Ti (w//b) increases at some fusion times, the Ti content in the TiO_2 product also increases. Based on Fig. 6(c), it can be seen that as the ratio of NaOH:Ti (w/w) increases at different particle sizes, the Ti content in the TiO_2 product also increases. However, from the three ratios of NaOH:Ti (w/w) used, it can be seen that the content of Ti significantly increased from the ratio NaOH:Ti (w/w) = 1:2 to 2:1, while from 2:1 to 4:1 there was

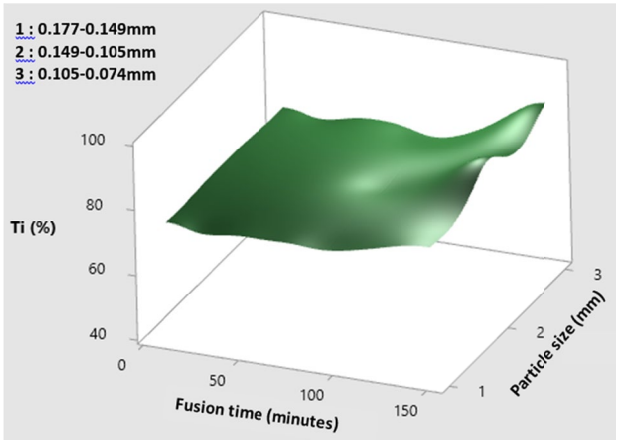

(a) Surface plot of Ti (%) vs particle size (mm), fusion time (minutes)

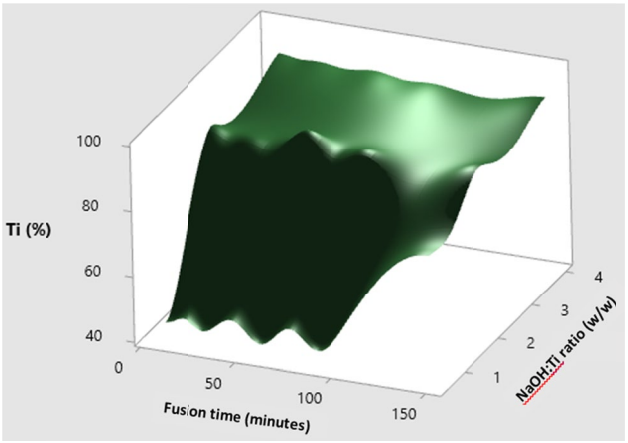

(b) Surface plot of Ti (%) vs NaOH:Ti ratio (w/w), fusion time (minutes)

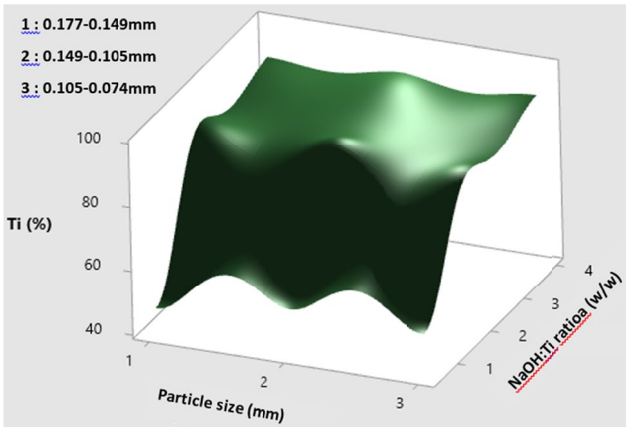

(c) Surface plot of Ti (%) vs NaOH:Ti ratio (w/w), particle size (mm)

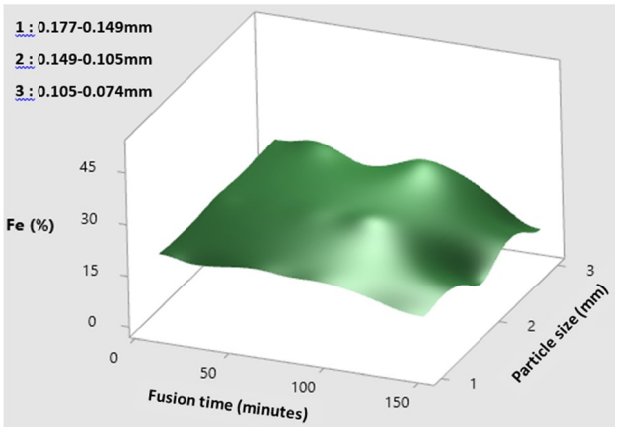

(d) Surface plot of Fe (%) vs particle size (mm), fusion time (minutes)

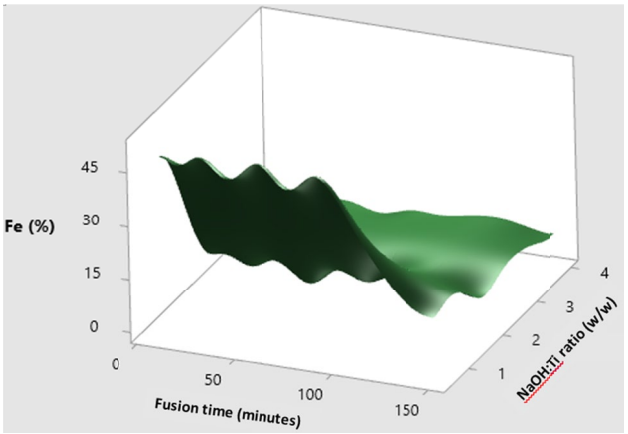

(e) Surface plot of Fe (%) vs NaOH:Ti ratio (w/w), fusion time (minutes)

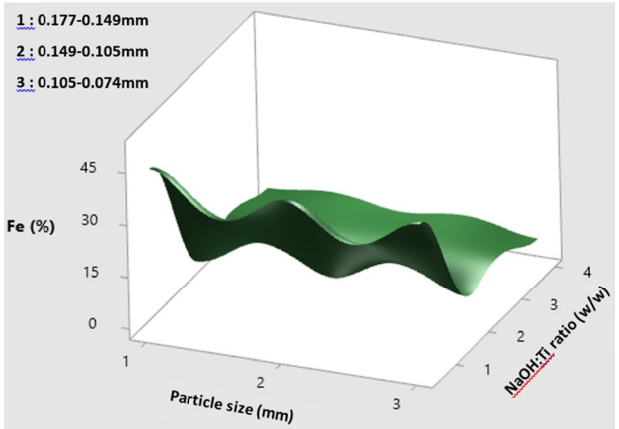

(f) Surface plot of Fe (%) vs NaOH:Ti (w/w) ratio, particle size (mm)

Fig. 6. Effect particle size, NaOH: Ti ratio, and fusion time to Ti and Fe content in TiO_2 product

not a significant increase in Ti contents in TiO_2 products. The effect of fusion time on Ti contents in TiO_2 products is shown in Fig. 6(a and b). In Fig. 6(a), it can be seen that as the fusion time increases, the Ti content in the TiO_2 product also increases for the three particle sizes used. Whereas in Fig. 6(b), it can be seen that the effect of time does not significantly affect the Ti content in the TiO_2 product at the several ratios used.

The effect of particle size on Fe content in TiO_2 products is shown in Fig. 6(d and f). Based on Fig. 6(d and f), it can be seen that the particle size has no effect on the Fe content in the TiO_2 product. The effect of the NaOH:Ti ratio (w/w) on the Fe content in the TiO_2 product is shown in Fig. 6(e and f). Based on Fig. 6(e and f), it can be seen that increasing the ratio of NaOH:Ti (w/w) during fusion with the same particle size reduces the Fe

content in the TiO_2 product, especially from the ratio NaOH:Ti (w/w) 1:2 to 2:1, while for the ratio of 2:1 to 4:1, the decrease is not too significant. The effect of fusion time on Fe content in TiO_2 products is shown in Fig. 6(d and e). In Fig. 6(d), it can be seen that as the fusion time increases, the Fe content in the TiO_2 product also tends to decrease for the three particle sizes used. Whereas in Fig. 6(e), it can be seen that the fusion time tends not to significantly affect the Fe content in the TiO_2 product at the several ratios used.

As an experimental control, all three particle sizes were roasted at 850°C for 150 minutes without NaOH to determine the effectiveness of the fusion process against Ti content in TiO_2 products. The use of hydrochloric acid is the same in both methods. TABLE 3 shows the Ti and Fe contents of TiO_2 products without adding NaOH. The content TiO_2 in products without NaOH is low, ranging from 38 to 43%. It is significantly different from the addition of NaOH 2:1 (NaOH: Ti) at the same fusion time, which results in the lowest resulting mean of TiO_2 in the product of 89.07%.

TABLE 3

Ti and Fe content XRF analysis on TiO_2 products without NaOH addition

Element	Content (% wt)		
	0.177-0.149 mm	**0.149-0.105 mm**	**0.105-0.074 mm**
TiO_2	39.816	43.611	38.214
Fe_2O_3	45.079	45.261	45.541

According to Fig. 7, the fusion process will alter the solid product's compound before continuing with the leaching process. Ilmenite and magnetite are the most abundant compounds in the raw materials. The predominant compounds in the fusion products at a NaOH: Ti = 1:2 ratio were sodium iron (III) titanium oxide ($NaFeTiO_4$), hematite (Fe_2O_3), and coesite (SiO_2). The fusion products of the dominant compound at a NaOH: Ti = 2:1 ratio are sodium iron titanate ($Na_{0.75}Fe_{0.75}Ti_{0.25}O_2$), sodium titanium oxide ($NaTiO_2$) and calcium iron oxide ($Ca_{2,5}Fe_{15,5}O_{25}$). The dominant compound resulting from fusion at the ratio NaOH:Ti = 4:1 is magnesioferrite (Fe_2MgO_4).

Foley and Mackinnon also discovered sodium iron titanate and sodium titanium dioxide. The mechanism of the observed reaction can be explained by reactions (1) to (3) [33,34]:

$$2\ Na_2O_{(l)} + 4\ FeTiO_{3\ (s)} + O_{2\ (g)} \rightarrow 4NaFeTiO_{4\ (s)} \quad (1)$$

$$6\ Na_2O_{(l)} + 12\ FeTiO_{3\ (s)} + \\ + 3\ O_{2\ (g)} \rightarrow 4NaFeTi_3O_{8\ (s)} + 8\ NaFeO_{2\ (s)} \quad (2)$$

$$14\ Na_2O_{(l)} + 12\ FeTiO_{3\ (s)} + \\ + 3\ O_{2\ (g)} \rightarrow 16\ Na_{0.75}Fe_{0.75}Ti_{0.25}O_{2\ (s)} + \\ + 8\ Na_2TiO_{3\ (s)} \quad (3)$$

The analysis showed that the NaOH: Ti = 1:2 ratio was only available in sufficient quantities to form $NaFeTiO_4$. Increasing the NaOH ratio causes the sodium ions (Na_2O) to melt, allowing reactions (2) and (3) to take place. Based on other studies' findings, the fusion process's overall reaction can be written at the reaction (4) [34-36].

$$28\ FeTiO_3 + 22\ Na_2O + \\ + 7\ O_2 \rightarrow 16\ Na_{0.75}Fe_{0.75}Ti_{0.25}O_2 + 3\ NaFeTiO_4 + \\ + 4\ Na_2Fe_2Ti_3O_{10} + 4\ Na_2TiO_3 + \\ + 2\ Na_8Ti_5O_{14} + 10\ NaFeO_2 \quad (4)$$

During the fusion reaction, contaminants like aluminum, chromium, silicon, phosphorus, vanadium, calcium, and magnesium are extracted. Sodium titanate and sodium ferrates might also be generated by the reaction [28]. The NaOH: Ti ratio of 2:1 had a purer TiO_2 product than the lower ratio, indicating that the alkali fusion process successfully separated the impurities from titanium.

Fig. 8 depicts the results of HSP processing, which show a phase transition from raw materials to TiO_2 products. Ilmenite and magnetite are the most abundant compounds in the raw material. The diffractogram of TiO_2 products at the NaOH: Ti = 1:2 (w/w) ratio reveals that the dominant compounds are sodium iron (III) titanate ($NaFeTiO_4$), andradite ($Ca_3Fe_{1.88}Si_3O_{12}$), and

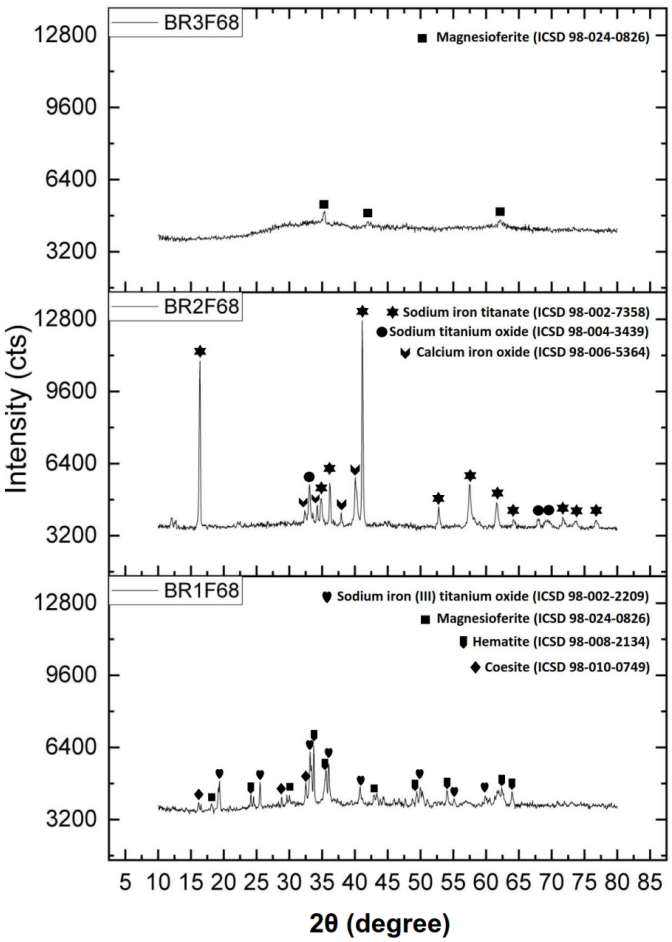

Fig. 7. XRD pattern of fusion product, BR1F6 (fusion with NaOH: Ti = 1:2 (w/w), t = 60 minutes), BR2F6 (fusion with NaOH:Ti = 2:1 ratio (w/w), t = 60 minutes), BR3F6 (fusion with NaOH:Ti = 4:1 ratio (w/w), t = 60 minutes)

coesite (SiO_2). The XRF analysis of TiO_2 products at a NaOH: Ti = 1:2 (w/w) ratio (Fig. 6(b,c)) revealed low Ti content while high Fe and other impurity content. The diffractograms TiO_2 products with ratios NaOH: Ti = 2:1 (w/w) and NaOH: Ti = 4:1 (w/w) shows the dominant compound is rutile (BR2AL6 and BR3AL6). The results of the XRF analysis (Fig. 6(a,b,c)) also showed the same thing where the content of Ti is already above 90%.

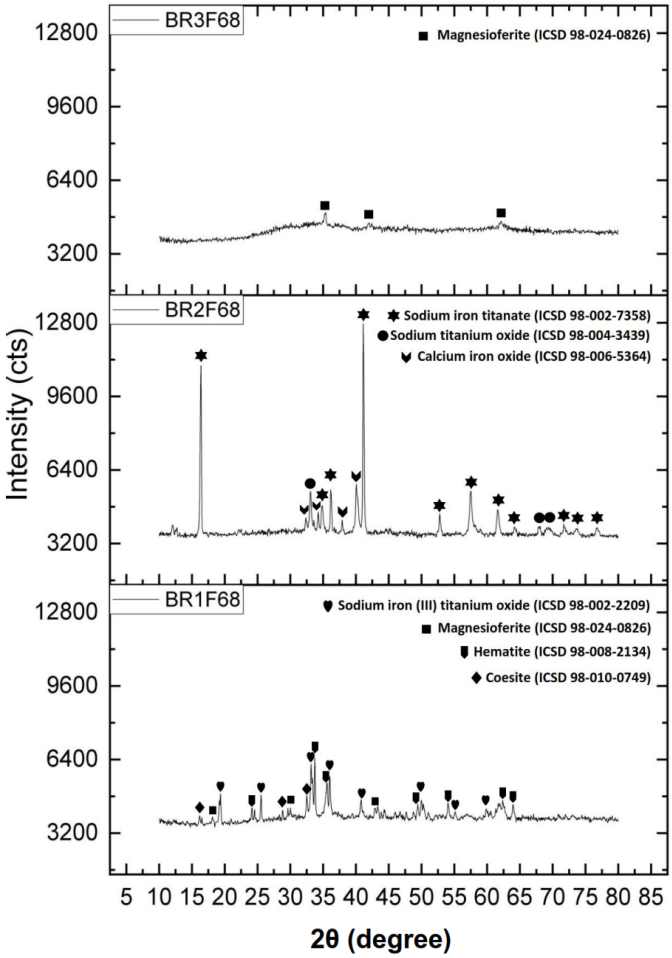

Fig. 8. XRD pattern of material (0.177-0.149 mm mesh) and TiO_2 product with NaOH: Ti ratio, BR1AL6 (fusion with NaOH:Ti = 1:2 (w/w), t = 60 minutes), BR2AL6 (fusion with NaOH:Ti = 2:1 ratio (w/w), t = 60 minutes), BR3AL6 (fusion with NaOH:Ti = 4:1 ratio (w/w), t = 60 minutes)

An increasing NaOH: Ti ratio (w/w) indicates an increasing Ti content in TiO_2 products (Fig. 6). The best results were obtained with a NaOH: Ti = 2:1 (w/w) ratio and a 60-minute fusion time. When fusing below the 2:1 mole ratio, 850°C produced ternary phases and sodium iron titanates [38]. At 850°C, the influence of fusion time has been investigated. Figs. 7 and 8 show that at a weight ratio of 1:2 (NaOH: Ti), the effect of fusion time on Ti contents on TiO_2 products is seen at a fusion time of 150 minutes for all particle sizes. As for the weight ratio of 2:1 and 4:1 (NaOH: Ti), fusion time does not significantly affect the content of Ti in TiO_2 products.

The SEM+EDS results in Fig. 9 confirmed that the NaOH: Ti ratio (w/w) significantly influences TiO_2 products. When the

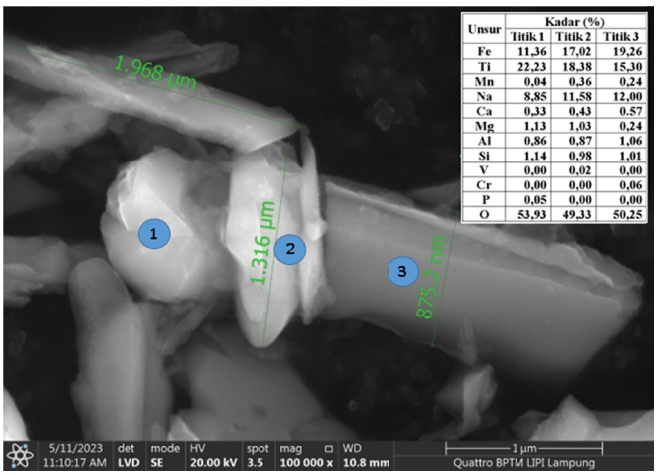

BR1P68 (fusion with NaOH: Ti = 1:2, t = 60 minutes)

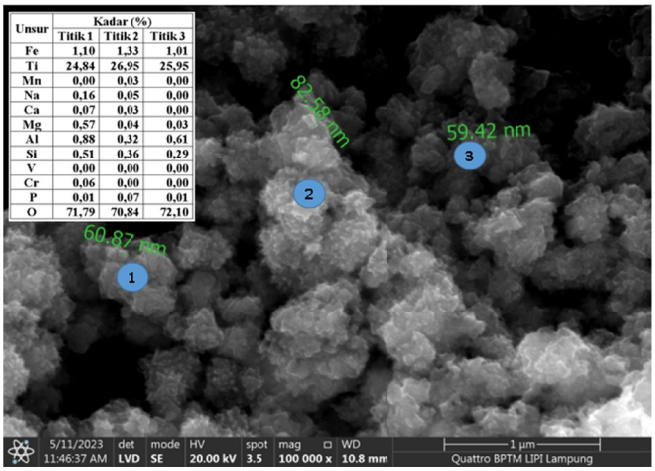

BR1P68 (fusion with NaOH: Ti = 2:1, t = 60 minutes)

Fig. 9. SEM+EDS analysis of TiO_2 product

NaOH: Ti (w/w) ratio is less than 2:1 (Fig. 9a), the TiO_2 product contains a high Fe content and impurities Al, Si, Na, and Ca. With a NaOH: Ti ratio of 2:1 (Fig. 9b), TiO_2 products are purer, with a Fe content of about 1% and minor impurities Al and Si. The alkaline fusion process aims to produce sodium iron titanate and extract water-soluble contaminants including aluminum, calcium, chromium, magnesium, phosphorus, vanadium, and silicon. The reaction produces water-soluble sodium silicate and sodium aluminate [9,30-2]. The conclusion is that the NaOH fusion process significantly impacts the Ti content of the products.

3.3.2. ANNOVA Analysis

Fig. 10 depicts the most influential variables in sequence are the ratio of NaOH: Ti (w /w), fusion time, and particle size. Fig. 10(a) shows the effect of the variable fusion time, particle size, and the ratio of NaOH:Ti (w/w) on the percentage of extraction of titanium (Ti), and Fig. 10(b) shows the effect of the variable fusion time, particle size, and the ratio of NaOH:Ti (w/w) on the percentage of extraction of titanium (Fe). The steeper the line that is formed, the greater the influence of the

variable. Likewise, the more sloping the line is, the smaller the influence of the existing variables. Based on the findings of this study, it is possible to conclude that low-grade ilmenite ore can be processed into TiO_2 with a Ti content ≥90%.

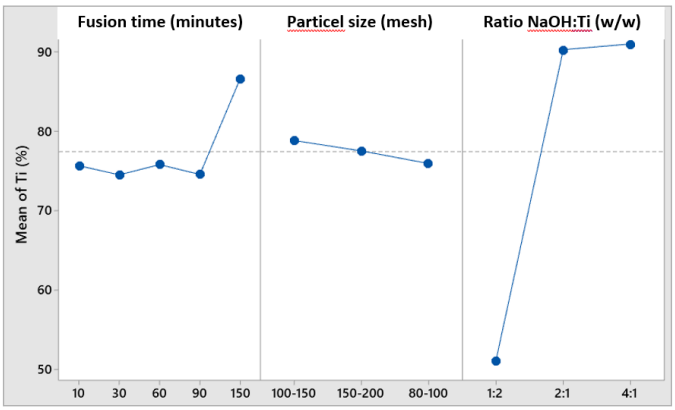

The main effect for Ti (% wt)

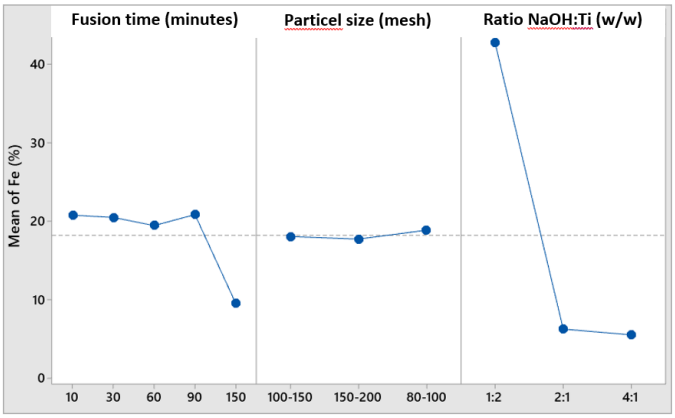

The main effect for Fe (% wt)

Fig. 10. The effects of variable time, particle size, and the ratio to percentage extraction of titanium and iron

4. Conclusions

The characterization of Banten low-grade ilmenite ore reveals that the dominant compounds are ilmenite ($FeTiO_3$), magnetite (Fe_3O_4), magnesioferrite (Fe_2MgO_4), and coesite (SiO_2). More than 85% of the particles were magnetic, according to the magnetization distribution for each particle size. The best conditions were 60 minutes of fusion at 850°C, a 2:1 NaOH: Ti ratio (w/w), and a 0.149-0.105 mm with 93.17% Ti in the product. According to Taguchi's analysis, the caustic fusion process significantly influences the resulting TiO_2 product more than particle size and fusion time.

Acknowledgments

We express our gratitude to the Research Center for Mining Technology-National Research and Innovation Agency (PRTPB-BRIN), Department of Chemical Engineering (Sustainable Mineral Processing Research Group), Faculty of Engineering, Gadjah Mada University for providing the facility and financial support for this study.

REFERENCES

[1] Y. Aristanti, Y.I. Supriyatna, N.P. Masduki, S. Soepriyanto, Decomposition of Banten Ilmenite by Caustic Fusion Process for TiO_2 Photocatalytic Applications. IOP Conf. Ser.: Mater. Sci. Eng. **285**, 012005 (2018).
DOI: https://doi.org/10.1088/1757-899X/285/1/012005

[2] Y. Aristanti, Y.I. Supriyatna, N.P. Masduki, S. Soepriyanto, Effect of Calcination Temperature on the Characteristics of TiO_2 Synthesized from Ilmenite and Its Applications for Photocatalysis. IOP Conf. Ser.: Mater. Sci. Eng. **478**, 012019 (2019).
DOI: https://doi.org/10.1088/1757-899X/478/1/012019

[3] Y.I. Supriyatna, S. Sumardi, W. Astuti, A.N. Nainggolan, A.W. Ismail, H.T.B.M. Petrus, A. Prasetya, Characterization and a Preliminary Study of TiO_2 Synthesis from Lampung Iron Sand. Key. Eng. Mat. **849**, 113-118 (2020).
DOI: https://doi.org/10.4028/www.scientific.net/KEM.849.113

[4] Y.I. Supriyatna, W. Astuti, S. Sumardi, Sudibyo, A. Prasetya, L.I.Br. Ginting, Y. Irmawati, N.S. Asri, H.T.B.M. Petrus, Correlation of Nano Titanium Dioxide Synthesis and the Mineralogical Characterization of Ilmenite Ore as Raw Material. Int. J. Tech. **12** (4), 749-759 (2021).
DOI: https://doi.org/10.14716/ijtech.v12i4.4270

[5] N.S. Awwad, H.A. Ibrahium, Kinetic extraction of titanium (IV) from chloride solution containing Fe(III), Cr(III), and V(V) using the single drop technique. J. Env. Chem. Eng. **1** (1-2), 65-72 (2013). DOI: https://doi.org/10.1016/j.jece.2013.03.009

[6] M.J. Gázquez, J.P. Bolívar, R. Garcia-tenorio, F. Vaca, A Review of the Production Cycle of Titanium Dioxide Pigment. Mater. Sci. and Apl. **5** (7), 441-458 (2014).
DOI: https://doi.org/10.4236/msa.2014.57048

[7] N.A. Jabit, G. Senanayake, Characterization and Leaching Kinetics of Ilmenite in Hydrochloric Acid solution for Titanium Dioxide Production. J. Phy. **1082** (1), 1-7 (2018).
DOI: https://doi.org/10.1088/1742-6596/1082/1/012089

[8] R. Razavi, S.M.A. Hosseini, M. Ranjbar, Production of Nanosized Synthetic Rutile from Ilmenite Concentrate by Sonochemical HCl and H_2SO_4 Leaching. Iran. J. Chem. Chem. Eng. **33** (2), 29-36 (2014).
DOI: https://doi.org/10.30492/IJCCE.2014.10749

[9] T. Xue, L. Wang, T. Qi, J. Chu, J. Qu, C. Liu, Decomposition kinetics of titanium slag in sodium hydroxide system. Hydrometallurgy **95**, 22-27 (2009).
DOI: https://doi.org/10.1016/j.hydromet.2008.04.004

[10] Y. Guo, S. Liu, T. Jiang, G. Qiu, F. Chen, A Process for Producing Synthetic Rutile from Panzhihua Titanium Slag. Hydrometallurgy **147-148**, 134-141 (2014).
DOI: https://doi.org/10.1016/j.hydromet.2014.05.009

[11] J.E. Kogel, N.C. Trivedi, J.M. Barker, S.T. Krukowski, Industrial Minerals and Rocks, Commodities, Markets and Uses. 7th ed. Littleton, Colorado, USA, 987-1003 (2006).

[12] K.N. Han, New Trends and Challenges in Leaching Process. Min. Proc. Ext. Met. Rev. **8** (1-4), 57-72 (1992). DOI: https://doi.org/10.1080/08827509208952678

[13] L. Jia, B. Liang, L. Lü, S. Yuan, L. Zheng, X. Wang, C. Li, Beneficiation of Titania by Sulfuric Acid Pressure Leaching of Panzhihua Ilmenite. Hydrometallurgy **150**, 92-98 (2014). DOI: https://doi.org/10.1016/j.hydromet.2014.09.016

[14] S. Middlemas, Z.Z. Fang, P. Fan, Life Cycle Assessment Comparison of Emerging and Traditional Titanium Dioxide Manufacturing Processes. J. Clean. Prod. **89**, 137-147 (2015). DOI: https://doi.org/10.1016/j.jclepro.2014.11.019

[15] U.S. Geological Survey. Mineral Commodity Summaries 2020. U.S. Government Publishing, Reston, VA, USA. (2020). DOI: https://doi.org/10.3133/mcs2020

[16] A. Jha, M.P. Antony, T.V. Dattatray, US Application Patent 20070110647 (2007).

[17] A. Lahiri, E.J. Kumari, A. Jha, Kinetic studies on the soda-ash roasting of titaniferous ores to extract TiO_2. Adv. Proc. Metals and Mater: Thermo and physicochemical principles: non-ferrous high-temperature processing **1**, 115-123 (2006).

[18] T. Laird, Ullman's Encyclopaedia of Industrial Chemistry, Vol. A28. 5th edition. VCH: Weinheim, Germany (1997).

[19] J.P. Van Dyk, N.M. Vegter, C.P. Visser, T. de Lange, J.D. Winter, E.A. Walpole, and J. Nell, Beneficiation of Titania Slag by Oxidation and Reduction Treatment. U.S. Patent 6 803 024 (2004).

[20] Z. Yuan, X. Wang, C. Xu, W. Li, M. Kwauk, A new process for comprehensive utilization of complex titania ore. Miner. Eng. **19** (9), 975-978 (2006). DOI: https://doi.org/10.1016/j.mineng.2005.10.002.

[21] S. Samanta, S. Mukherjee, R. Dey, Oxidation behavior and phase characterization of titaniferous magnetite ore of Eastern India. T. Nonferr. Metal. Soc. **24** (9), 2976-2985 (2014). DOI: https://doi.org/10.1016/S1003-6326(14)63434-8

[22] A. Mehdilo, M. Irannajad, B. Rezai, Applied mineralogical characterization of ilmenite from Kahnuj placer deposit, Southern Iran. Period. Miner. **84** (2), 289-302 (2015). DOI: https://doi.org/10.2451/2015PM0014

[23] T. Grammatikopoulos, A. Mcken, C. Hamilton, O.A. Christiansen, Vanadium-bearing magnetite and ilmenite mineralization and beneficiation from the Sinarsuk V-Ti project. West Greenland. CIM Bull. **95**, 87-95 (2002).

[24] Z. Zhu, W. Zhang, C.Y. Cheng, A literature review of titanium solvent extraction in chloride media. Hydrometallurgy **105** (3-4), 304-313 (2011). DOI: https://doi.org/10.1016/j.hydromet.2010.11.006

[25] L. Zhang, H. Hu, Z. Liao, Q. Chen, J. Tan, Hydrochloric acid leaching behavior of different treated Panxi ilmenite concentrations. Hydrometallurgy **107** (1-2), 40-47 (2011). DOI: https://doi.org/10.1016/j.hydromet.2011.01.006

[26] N.A. Jabit, Chemical and Electrochemical Leaching Studies of Synthetic and Natural Ilmenite in Hydrochloric Acid Solutions, Murdoch University 1-303 (2017).

[27] L. Chen, S. Wen, G. Xu, H. Xie, A Novel Process for Titanium Sand By Magnetic Separation and Gravity Concentration. Min. Proc. Ext. Met. Rev. **34** (3), 139-150 (2013). DOI: https://doi.org/10.1080/08827508.2011.623749

[28] W. Hoecker, Process for the production of synthetic rutile. European Patent EP0612854 (1994).

[29] H.N. Sinha, The Murso synthetic rutile process. Light Metals 367-373 (1975).

[30] M. Robinson, F. Clamp, D.B. Mobbs, R.V. Pearse, The Laporte high-efficiency ilmenite beneficiation process. In: Jones M.J. (Ed.), Adv. Ext. Met. IMM. p. 89-96, London (1977).

[31] S. Kataoka, S. Yamada, Acid leaching upgrades ilmenite to synthetic rutile. Chem. Eng. **80** (7), 92-93 (1973).

[32] E.A. Walpole, J.D. Winter, The Austpac ERMS and EARS processes for the manufacture of high-grade synthetic rutile by the hydrochloride leaching of ilmenite. Proceedings of Chloride Metallurgy 2002, 2. Montreal, Canada, p. 401-415 (2002).

[33] A.J. Manhique, Titania Recovery from Low-grade Titaniferrous Minerals (Ph.D dissertation]. University of Pretoria 1-128 (2012). DOI: http://hdl.handle.net/2263/24305

[34] E. Foley, K.P. Mackinnon, Alkaline roasting of ilmenite. J. Sol. State Chem. **1**, 566-575 (1970).

[35] C. Li, A.F. Reid, S. Saunders, Nonstoichiometric alkali ferrites and aluminates in the systems $NaFeO_2$–TiO_2, $KFeO_2$–TiO_2, $KAlO_2$–TiO_2, $KAlO_2$–SiO_2. J. Sol. State Chem. **3**, 614-620 (1971). DOI: https://doi.org/10.1016/0022-4596(71)90109-5

[36] A.F. Reid, M.J. Sienko, Some characteristics of sodium titanium bronze and related compounds. Inorg. Chem. **6** (2), 321-324 (1967). DOI: https://doi.org/10.1021/ic50048a028

[37] M.J. Hollit, R.A. McClelland, J.R. Tuffley, Upgrading titaniferous materials. US Patent No. 20030129113 (2003).

[38] T.A.I. Lasheen, Chemical benefication of Rosetta ilmenite by direct reduction leaching. Hydrometallurgy **76**, 123-129 (2008). DOI: https://doi.org/10.1016/j.hydromet.2004.10.002

[39] LA. Yousef, Upgrading of TiO_2 Separated from Ilmenite Mineral, Rosetta, Black Sands of Egypt. Arab Journal of Nuclear Science and Aplications **48** (4), 33-43 (2015).

[40] L. Trivana, S. Sugiarti, E. Rohaeti, Synthesis and characterization of sodium silicate (Na_2SiO_3) from rice husk. J. Environ. Sci. Tech. **7** (2), 66-75 (2015).

[41] N.H.M. Zhely, N. Widiastuti, Synthesis of X-carbon Zeolite from Coalbed Ash and Its Characterization as a Hydrogen Storage Material. Proceedings of Chemistry FMIPA–ITS. Surabaya, Indonesia (2012).